

Nanoscale

Accepted Manuscript



This is an *Accepted Manuscript*, which has been through the Royal Society of Chemistry peer review process and has been accepted for publication.

Accepted Manuscripts are published online shortly after acceptance, before technical editing, formatting and proof reading. Using this free service, authors can make their results available to the community, in citable form, before we publish the edited article. We will replace this *Accepted Manuscript* with the edited and formatted *Advance Article* as soon as it is available.

You can find more information about *Accepted Manuscripts* in the [Information for Authors](#).

Please note that technical editing may introduce minor changes to the text and/or graphics, which may alter content. The journal's standard [Terms & Conditions](#) and the [Ethical guidelines](#) still apply. In no event shall the Royal Society of Chemistry be held responsible for any errors or omissions in this *Accepted Manuscript* or any consequences arising from the use of any information it contains.



Role of the cell cycle on the cellular uptake of folate-modified poly(L-amino acids) micelles in a cell population

Received 00th January 20xx,
Accepted 00th January 20xx

Jihui Tang^a, Ziwei Liu^a, Fenqi Ji^a, Yao Li^a, Junjie Liu^a, Jian Song^a, Jun Li^{a†}, Jianping Zhou^{b†}

DOI: 10.1039/x0xx00000x

www.rsc.org/

Nanoparticles are widely recognized as a vehicle for tumor-targeted therapies. There are many factors that can influence the uptake of nanoparticles, such as the size of the nanoparticles, and/or their shape, elasticity, surface charge and even the cell cycle phase. However, the influence of the cell cycle on the active targeting of a drug delivery system has been unknown until now. In this study, we initially investigated the folate receptor α (FR- α) expression in different phases of HeLa cells by flow cytometric and immunocytochemical methods. The results obtained showed that FR- α expression was cell cycle-dependent, i.e. the S cells folate receptor expression was highest as the cell progressed through its cycle. Then, we used folate modified poly(L-amino acids) micelles (FA-PM) as an example to investigate the influence of the cell cycle on the active targeting drug delivery system. The results obtained indicated that the uptake of FA-PM by cells was influenced by the cell cycle phase, and the S cells took up the greatest number of folate conjugated nanoparticles. Our findings suggest that future studies on ligand-mediated active targeting preparations should consider the cell cycle, especially when this system is used for a cell cycle-specific drug.

Introduction

Nanoparticles with a nanometer size are taken up by cells more easily than larger molecules¹, and they can be distributed to the tumor tissue depending on the enhanced permeability and retention (EPR) effect and enter tumor cells by energy-dependent pathways. Nano-drug delivery systems have been extensively studied for use with targeted therapies. Many studies have shown that the cellular uptake and intracellular distribution of nanoparticles depend on many factors, including the size and/or shape, elasticity, surface charge and surface properties²⁻⁶.

The effect of specific aspects of the nanoparticles on cellular uptake has been widely studied including cell changes in the process of mitosis in mammalian cells, such as the shape⁷, membrane tension⁸, protein expression⁹, cell volume, and viscosity¹⁰. Several studies have shown that these factors can have an impact on the cellular uptake. For example, the cell volumes and apparent viscosities of GAP A3 hybridoma cells increased by a factor of 3 to 4 during the cell cycle progression⁷. Many studies have shown that membrane protein¹¹, glucose regulated protein¹², Nerve Growth Factor Receptors¹³, surface antigens¹⁴⁻¹⁶, CXCR chemokine receptors¹⁷, LA350 surface actin⁹ and even the membrane composition¹⁸ fluctuated with the cell cycle.

Considering these changes during the cell cycle, the effects of the cell cycle on nanoparticle uptake were investigated. Zheng *et al.*, synthesized water-soluble quantum dots (QDs), i.e. thiol-capped

CdTe QDs, and the cellular uptake of QDs in the HeLa cells was studied by laser scanning confocal microscopy. The fluorescence of QDs in the G2/M phase was much more intense than that in the S phase, and a quantitative study by flow cytometry indicated that the uptake of thiol-capped QDs by HeLa cells in the G2/M phase was nearly twice that in the S phase¹⁹. Kim *et al.*, studied the uptake of fluorescent labelled carboxylated polystyrene (PS-COOH) in different phases of A549 cells (human lung carcinoma). The results obtained indicated that nanoparticles were internalized at similar rates in different phases of the cell cycle. However, after 24 h, the concentration of nanoparticles in the different phases of the cell cycle could be ranked: G2/M > S > G0/G1. This is because the concentration of internalized nanoparticles was diluted when the parent cell divides into daughter cells during the cell cycle²⁰. Åberg *et al.*, developed a theoretical framework for the nanoparticle uptake and accumulation kinetics in dividing cell populations²¹.

The most recent studies have mainly concentrated on the passive uptake of nanoparticles affected by the cell cycle. However, currently, ligands (such as folate) involving conjugated nanoparticles are now important active targeted drug delivery strategies for cancer therapy²²⁻²⁴. The use of folate ligands as a targeting device is due to the fact that folate receptors are overexpressed in many human cancer cells, some are even 100-300 times higher than that observed in normal tissues²⁵. Therefore, in this study, we initially investigated the changes in folate receptor expression during the cell division cycle in a human cervical carcinoma cell line (HeLa) by flow cytometric and immunocytochemical methods. Then, the fluorescein isothiocyanate (FITC) loaded folate modified poly(L-amino acids) micelles taken up by the different phases of HeLa cells were studied by laser scanning confocal microscopy and flow cytometry.

Results and discussion

^aSchool of Pharmacy, Anhui Medical University, 81 Meishan Road, Hefei 230032, China.

^bDepartment of Pharmaceutics, China Pharmaceutical University, 24 Tongjiaxiang, Nanjing 210009, China.

† Corresponding author.

lijun@ahmu.edu.cn (Jun Li), Tel./fax: +86 0551 65161115.

zhoujpcpu@126.com (Jianping Zhou), Tel./fax: +86 025 83271272

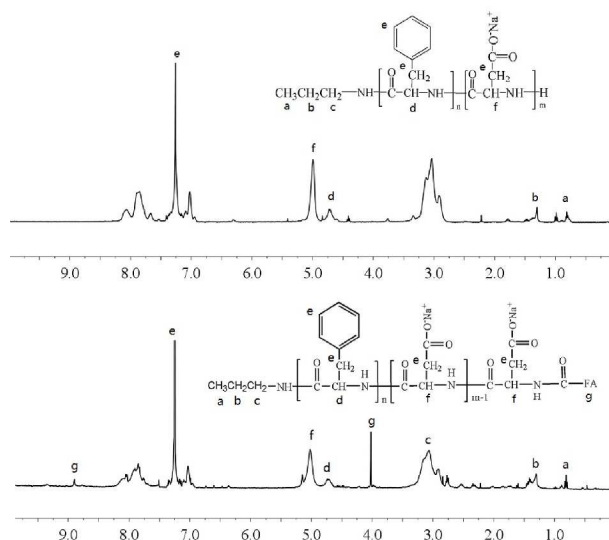


Figure 1. ^1H NMR spectrum of PAA-PPA and FA-PAA-PPA.

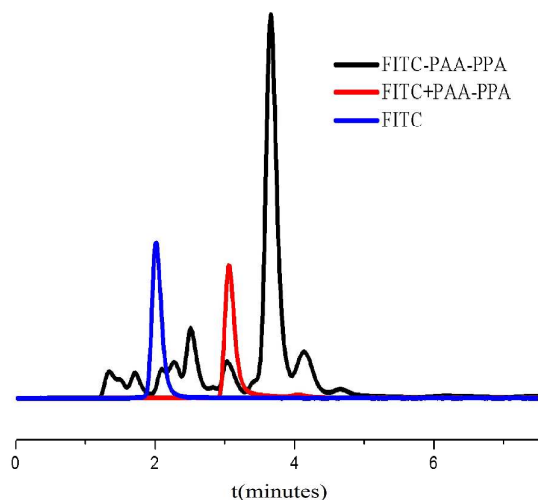


Figure 2. HPLC chromatograms of FITC (blue line), FITC-PAA-PPA (black line), and FITC + PAA-PPA (red line).

Synthesis of poly(L-aspartic acid)-b-poly(L-phenylalanine) (PAA-PPA) and folate-modified PAA-PPA (FA-PAA-PPA)

Confirmed by ^1H NMR spectrometry, the synthesized PAA-PPA and FA-PAA-PPA (Figure 1). The degree of PAA polymerization was calculated from the integrated value ratio of the $-\text{CH}-$ proton signal (4.98 ppm) to the $-\text{CH}_3$ proton signal (0.81 ppm), while the degree of PPA polymerization was calculated from the $-\text{CH}-$ proton signal (4.69 ppm) and the $-\text{CH}_3$ proton signal²⁶. The degree of folate substitution was calculated by the integrated value of 8.89 ppm and 4.01 ppm of the folate proton signal to the $-\text{CH}_3$ proton signal. In this study, the degree of substitution of folate was about 71.5%.

In this study, due to the proton signal of FITC between 6.0 and 7.0 was overlapped with that of PAA-PPA, the FITC-PAA-PPA was confirmed by HPLC chromatogram according to Wang, C. *et al.*²⁷ FITC was conjugated to the $-\text{NH}_2$ of PAA-PPA through its $\text{N}=\text{C}=\text{S}$, and the HPLC chromatogram is shown in Figure 2. In this study, the

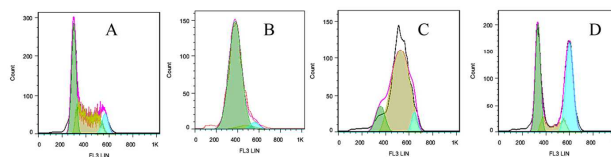


Figure 3. Cell cycle of synchronicity of HeLa cells. (A) Normal group; (B) Cells were arrested at the G1 phase; (C) Cells were arrested at the S phase; (D) Cells were arrested at the G2/M phase.

Table 1. Cell cycle data of synchronicity of HeLa cells (n=3)

Cell-cycle phase distribution	Normal Group (%)	synchronization percentage (G1)	synchronization percentage (S)	synchronization percentage (G2/M)
G1	42.9±0.9	87.1±2.1**	14.2±1.7	37.6±4.7
S	39.51±0.9	7.9±4.8	71.8±8.5**	11.4±1.2
G2/M	11.9±0.6	2.4±2.1	6.2±0.1	44.1±4.6**

** Significantly different from the Normal group ($P < 0.01$).

retention time of the FITC was 2.1 minutes (which is slightly more than the dead time of this HPLC system.) and, the retention time of the FITC and PAA-PPA mixture was 3.1 minutes, while that the retention time of FITC-PAA-PPA was 3.7 minutes, which was greater than that of the FITC and PAA-PPA mixture (FITC/PAA-PPA). This may be due to FITC in FITC/PAA-PPA penetration into the PAA-PPA micelles, and through a physical interaction, while that the FITC in FITC-PAA-PPA did not involve a physical interaction but a covalent bond. Following the preparation of FITC-PAA-PPA, it was dialyzed against deionized water until the dialysate was no longer green, and it was believed that the FITC did not leak out during the experimental process. Therefore, FITC-PAA-PPA is suitable for determining the cellular uptake of micelles.

Cell-cycle phase distribution

To investigate the effect of the cell cycle phase on the uptake of micelles, HeLa cells were synchronized by a classical double thymidine block. To determine the relative position of the sites of arrest by thymidine, we used flow cytometry to measure the cellular DNA content. After a double thymidine block, 87.1% of the cells were arrested at the G1/S boundary. Upon release from the thymidine block, 71.8% of the cells progressed to the S phase (4 h), and 44.1% entered the G2/M phase (10 h). The synchronized cells of the G1, S and G2/M groups at the G1, S and G2/M phase increased significantly compared with the control group (see Figure 3 and Table 1). These results indicated that synchronized cells can be used to study the expression of folate receptors in different phases of the cell cycle.

Expression of folate receptors in different phases of the cell cycle

The folate-mediated tumor-specific drug delivery system has been extensively studied due to the folate receptor being overexpressed in many human cancer cells and the nanoparticles become internalized via an endocytic process when folate binds to its receptors. There are three major forms of folate receptor (FR): FR- α , FR- β and FR- γ . FR- α is over-expressed in malignant tissues and weakly expressed in normal tissues and, due to its higher affinity for folic acid and physiologic folates compared with FR- β and FR- γ , we focussed on the expression of FR- α in different phases of HeLa cells²². For intuitive observation of the expression of FR- α , Immunohistochemistry (IHC) was used to study the FR- α in different phases of

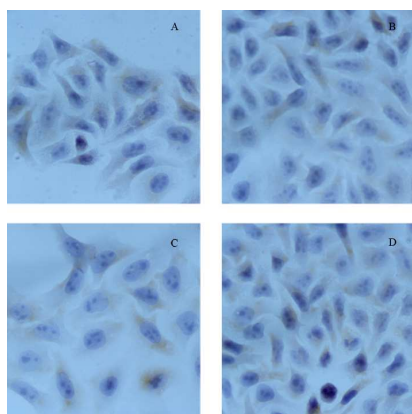


Figure 4. The IHC picture of the expression of folate receptors in different cell cycle phases (Immunohistochemistry $\times 200$). (A) Cells were arrested at the G1 phase; (B) Cells were arrested at the S phase; (C) Cells were arrested at the G2/M phase; (D) Normal group;

Table 2. Flow cytometry data on the expression of folate receptors in different cell cycle phases (n=3).

Phase	Flow cytometry	
	Expression percentage	Mean PL intensity
Synchronicity (G1)	82.2 \pm 11.3	1.9 \pm 0.9 \times 10 ⁴
Synchronicity (S)	93.2 \pm 6.5	2.8 \pm 0.7 \times 10 ⁴ **
Synchronicity (G2/M)	80.0 \pm 9.5	0.9 \pm 0.1 \times 10 ⁴
Normal	84.5 \pm 5.5	1.1 \pm 0.1 \times 10 ⁴

** Significantly different from the Normal group (P < 0.01).

HeLa cells (shown in Figure 4). From Figure 4, we can see that it is yellow in the cell membrane and cytoplasm, which means that FR- α is expressed not only in the cell membrane but also in the cytoplasm. Moreover, flow cytometry was used as a quantitative analysis method in this study. As can be seen from Figure 5 and Table 2, the percentage expression of FR- α was higher at 93.2% in the S phase, which was more than in the G1, and G2/M phase and in normal cells. The mean photoluminescence (PL) intensity of flow cytometry picture in the S phase was higher than that in the G1, and G2/M phase and in normal cells. What's more, in the process of flow cytometry analysis, the cell membrane is not be destroyed, so the measuring result of flow cytometry demonstrated only the part of the receptor that is at the cell membrane.

All these findings suggest that the drug delivered with folate as the targeting ligand will differ depending on the phase of the cell cycle. To verify this, we used FITC-modified poly(L-aspartic acid)-b-poly(L-phenylalanine) micelles (FI-PM) to study the effects of different phases of the cell cycle on the uptake of micelles.

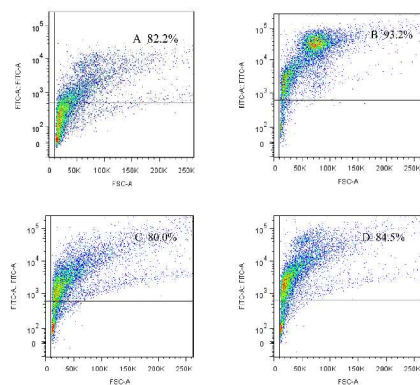


Figure 5. Flow cytometry analysis of the expression of FR- α in different cell cycle phases. (A) Cells were arrested at the G1 phase; (B) Cells were arrested at the S phase; (C) Cells were arrested at the G2/M phase; (D) Normal group;

Effects of different phases of the cell cycle on the uptake of micelles

Confocal fluorescence images of different phases of HeLa cells treated with green fluorescent PAA-PPA micelles are shown in Figure 6. From Figure 6, we can see that all the groups had a green fluorescence, and the fluorescence distribution is localized on the cell membrane and cytoplasm, mainly on the cell membrane. This indicated that the micelles can be taken up by HeLa cells. The micelles were mainly on the cell membrane, only a small fraction was intracellular. This may be due to the cells being treated with micelles for only 1h, and the cells did not have enough time to transport the micelles intracellularly. In this study, considering the cell mitosis during the cell uptake experiments, the cells were treated with micelles for only 1h.

Compared with FI-PM, as a whole, the cells treated with folate-modified poly(L-aspartic acid)-b-poly(L-phenylalanine) micelles (FA-PM) have a stronger fluorescence, which means that the cells took up more FA-PM than FI-PM. To better quantify the uptake of FI-PM and FA-PM, the cells were exposed to the micelles and the fluorescence of these samples was assessed by flow cytometry. Representative flow cytometry distributions of cell fluorescence intensity in different phases of cells exposed to FI-PM and FA-PM are given in Figure 7 and Table 3. As we can see from Figure 7 and Table 3, all the groups exhibit a high percentage uptake. The percentage uptake and mean PL intensity of the synchronicity G2/M group treated with FI-PM were 87.5% and 26.6, respectively, which was higher than the synchronicity G1 group and S group. In addition, the percentage uptake and mean PL intensity of cells treated with FA-PM were higher than that of those treated with FI-PM and, after treatment with FA-PM, the percentage uptake and mean PL intensity of the synchronicity S group was the highest when compared with the synchronicity G1 and G2/M group. However, the percentage uptake and mean PL intensity decreased when folate was added to the cell culture medium, especially the uptake percentage of synchronicity S group decreased from 98.9% to 80.8%.

Table 3. Flow cytometry data of the uptake micelles in different cell cycle phases (n=3)

		Normal	Synchronicity (G1)	Synchronicity (S)	Synchronicity (G2/M)
PM (cell culture with 4 mM folate)	uptake percentage	50.3± 8.3	68.9± 9.4	70.8± 7.7	87.5± 10.3
	Mean PL intensity	16.5± 3.9	10.8± 2.4	10.2± 3.3	26.6± 8.1
FA-PM (cell culture without folate)	uptake percentage	75.6± 6.6**	87.1± 7.0*	98.9± 0.8**	89.8± 7.5
	Mean PL intensity	22.2± 4.5	13.6± 1.8	75.9± 14.2**	36.1± 3.6
FA-PM (cell culture with 4 mM folate)	uptake percentage	54.2± 4.3	72.6± 8.4	80.8± 8.1	85.6± 12.8
	Mean PL intensity	16.5± 3.2	11.8± 1.5	18.2± 1.3*	29.1± 9.3

* Significantly different from the Normal group (P < 0.05);

** Significantly different from the Normal group (P < 0.01).

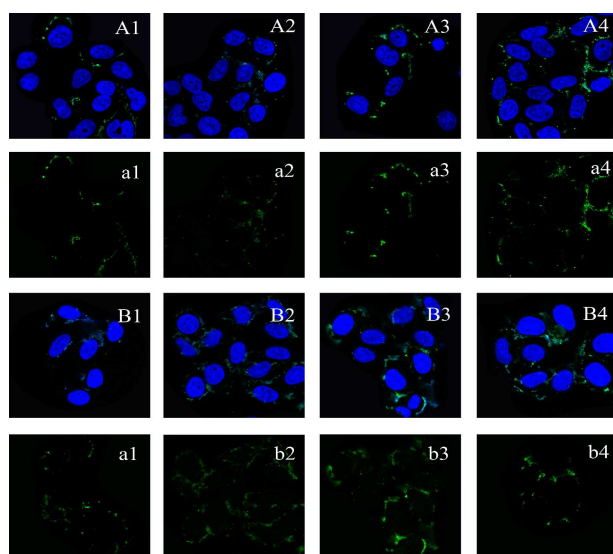


Figure 6. Confocal images of different phases of HeLa cells treated with green fluorescent PAA-PPA or FA-PAA-PPA micelles for 1 h. Blue: DAPI stained nuclei. A1-A4 treated with FI-PM (correspondingly, a1-a4 were the confocal images of green fluorescence channel): (A1, a1) normal group sample; (A2, a2) synchronicity of G1 group sample; (A3, a3) synchronicity of S group sample; (A4, a4) synchronicity of G2/M group sample; B1-B4 treated with FA-PM (correspondingly, b1-b4 were the confocal images of green fluorescence channel): (B1, b1) normal group sample; (B2, b2) synchronicity of G1 group sample; (B3, b3) synchronicity of S group sample; (B4, b4) synchronicity of G2/M group sample.

In this study, the synchronicity G2/M phase cells take up more FI-PM. This was in agreement with the report showing that, after 24 h, the G2/M phase cells internalized the most PS-COOH nanoparticles compared with G1 and S phase cells¹⁹. Another study indicated that the rate of uptake of thiol-capped CdTe QDs in the G2/M phase was 2-4 times higher than that in the G1 phase for HeLa, QGY7701 and the 293T cell line¹⁸. This may due to an increased membrane expansion during mitosis²⁶.

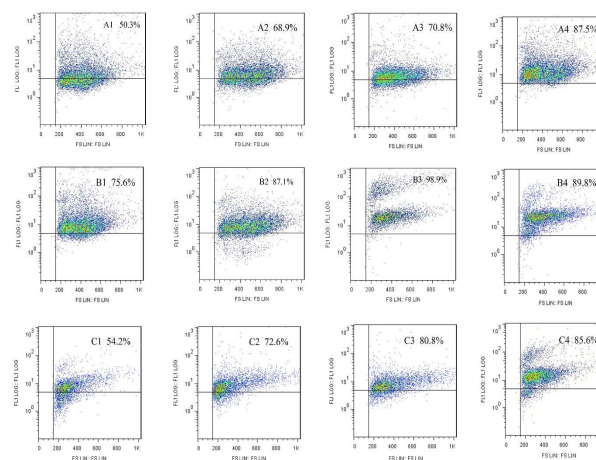


Figure 7. Flow cytometry of different phases of HeLa cells treated with green fluorescent PAA-PPA or FA-PAA-PPA micelles for 1 h. A1-A4 treated with FI-PM (cell culture with 4 mM folate): (A1) normal group sample; (A2) synchronicity G1 group sample; (A3) synchronicity S group sample; (A4) synchronicity G2/M group sample; B1-B4 treated with FA-PM (cell culture without folate): (B1) normal group sample; (B2) synchronicity G1 group sample; (B3) synchronicity S group sample; (B4) synchronicity G2/M group sample; C1-C4 treated with FA-PM (cell culture with 4 mM folate): (C1) normal group sample; (C2) synchronicity G1 group sample; (C3) synchronicity S group sample; (C4) synchronicity G2/M group sample.

The synchronicity S group uptake the most FA-PM in medium lacking folates, and this was consisted to the results that the synchronicity S group expression the highest folate receptor (see part 3.2). This may due to the uptake of FA-PM via folate receptor-mediated endocytosis, when the cells culture with folate, the folate receptor was saturated, the folate receptor-mediated endocytosis was restrain. So, the G2/M phase cells take up the most FA-PM in folates containing medium.

These results suggest that when we use folate-mediated drug delivery system to deliver a cell cycle-specific drug, such as Vinca alkaloids, paclitaxel, and Camptothecin (G2-M phase arrest)²⁹, the antitumor effect will be affected.

Experimental

Materials

The HeLa cell line was kindly provided by Dr. Yuxian Shen at the School of Basic Medical Sciences of Anhui Medical University; Dulbecco's modified Eagle's medium (DMEM) was purchased from Gibco Corporation; Thymidine was purchased from USB Corporation; Folate was purchased from Shanghai Yuan Ju Biological Technology Co., Ltd.; 35 mm Glass Bottom Cell Culture Dishes were purchased from NEST Biotechnology Co. LTD (Wuxi, China); FITC and 4',6-diamidino-2-phenylindole (DAPI) was obtained from Sigma (Shanghai, China). Human FOLR1 Antibody (Source: Monoclonal Mouse IgG1) was purchased from R&D Systems, Inc. Biotin-Streptavidin HRP Detection Systems and Fluorescein-Conjugated AffiniPure Goat Anti-Mouse IgG (H+L) were purchased from Beijing Zhongshan Jinqiao Biotechnology Co., Ltd. (Beijing, China).

Synthesis of PAA-PPA and FA-PAA-PPA

Poly(L-aspartic acid)-b-poly(L-phenylalanine) (PAA-PPA) was synthesized as previously reported²⁶. Briefly, before polymerization, L-phenylalanine NCA was reacted with an excess of n-propylamine as the initiator and the product was precipitated in excess diethyl ether. The white powder obtained and L-aspartic acid-benzyl ester NCA were dissolved in anhydrous DMF and stirred for 1 day at room temperature. The reaction mixture was then precipitated in diethyl ether and poly(L-aspartic acid-benzyl ester)-b-poly(L-phenylalanine) (PBAA-PPA) was obtained by filtration.

To synthesize FA-PAA-PPA, the carboxyl group of folic acid (110 mg, 0.25 mmol) was activated using N, N-dicyclohexylcarbodiimide (DCC, 0.3 mol)/N-hydroxysuccinimide (NHS, 0.3 mmol) in 5ml anhydrous dimethyl sulfoxide (DMSO) in the presence of 60 μ L triethylamine in the dark for 24 h at room temperature. After filtration, the reaction solution containing folate N-hydroxysuccinimidyl ester (folate-NHS) was incubated with PBAA-PPA (122 mg, 0.125 mmol) for 24 h. The resulting solution was then dialyzed against deionized water for 24 h. After filtration and lyophilization, the product was stirred in 1 M NaOH aqueous solution for 2 h and then dialyzed against deionized water for 24 h. After two days of freeze drying, FA-PAA-PPA was collected. To synthesize PAA-PPA, PBAA-PPA was stirred in 1M aqueous NaOH for 2 h to achieve debenzoylation, and then dialyzed against deionized water for 24 h followed by freeze drying. The FA-PAA-PPA, PAA-PPA was confirmed using a 400 MHz ¹H NMR spectrometer (Bruker, Switzerland)³⁰.

Synthesis of FITC-PAA-PPA

For this, 0.6 g(0.617 mmol) PBAA-PAA was treated with 24 mg(61.7 mmol) flu-orescein isothiocyanate (FITC) (sigma) in 15 mL diisopropylethylamine(DIEA)/DMF (20% v/v) overnight. The reaction solution was dialyzed against deionized water for 48 h followed by freeze drying. The product was stirred in 1M aqueous NaOH solution for 2h and dialyzed against deionized water, until the dialysate was no longer green, to obtain FITC-PAA-PPA²⁷. Then, the product was analyzed using RP-HPLC with a mobile phase consisting of methanol: water(60: 40), involving the use of a Shimadzu LC-20AT pump, an SIL-20A autosampler, a CTO-10AS column oven, and an RF-10AXL fluorescence detector and a Hypersil ODS2 column (150 \times 4.6 mm, 5 μ m, Dalian Elite Analytical

Instruments Co. Ltd., China). The Ex. and Em. wavelengths were set at 492 nm and 518 nm, respectively.

Preparation of FI-PM and FA-PM micelles

FI-PM were prepared by dissolving the PAA-PPA and FITC-PAA-PPA (1: 1, weight ratio) in 0.01M pH7.4 phosphate-buffered saline (PBS) at a concentration of 1 mg/mL. FA-PM were prepared by dissolving the mixture of FA-PAA-PPA and FITC-PAA-PPA (1: 1, weight ratio) in 0.01M pH7.4 PBS at a concentration of 1 mg/mL²⁶.

Cell synchronization

To obtain G0/G1, S and G2/M cell enriched cultures, HeLa cells were plated and, at 25-30% confluence, washed twice with 1 \times PBS followed by the addition of fresh DMEM + 2mM thymidine for 18 h (first block). After the first thymidine block, the thymidine was removed by washing with 1 \times PBS and fresh DMEM was added for 9 h to release the cells. After release, fresh DMEM and 2 mM thymidine was added for 17 h (second block). After the second block, the cells entered the G0/G1 phase. Then, thymidine was removed by washing with 1 \times PBS and fresh DMEM was added, and the culture was continued for 4 h(S phase) and 10 h(G2/M phase). Cell synchronicity was monitored by flow cytometry of the propidium iodide-stained cells. The flow cytometry data were collected for each of the three independent samples in this study³¹.

Folate Receptor-a Analysis³²

Cells were digested with 0.25% Pancreatin, and centrifuged at 1200 rpm, 4 $^{\circ}$ C, for 5 minutes, washed twice with precool 2% BSA followed by the addition of 3 μ L mouse anti-human monoclonal antibody FOLR1 1: 30, and incubated for 40 minutes at 4 $^{\circ}$ C. Then, 3 μ L mouse IgG was added to the isotype control group. After further washing, the samples were incubated with 5 μ L FITC-labeled Goat Anti-Mouse IgG 1: 30 for 40 minutes at 4 $^{\circ}$ C. They were then washed and fixed in 0.5 ml 4% paraformaldehyde prior to analysis using a BD FACSVerser flow cytometer. Data were analyzed off-line using FlowJo 7.6.1.

Cells were cultured in six-well culture plates fitted with coverslips, washed twice with 0.01 M PBS, and incubated with mouse anti-human monoclonal antibody FOLR1 1: 300 overnight at 4 $^{\circ}$ C. Immunohistochemistry (IHC) was performed using an SPlink Detection Kit (Beijing Zhongshan Jinqiao Biotechnology Co., Ltd., Beijing, China) as previously described³³.

Cell culture and micelle treatments³⁴

The HeLa cell line was grown on Glass Bottom Cell Culture Dishes or 6 well cell culture clusters in DMEM containing 10% fetal bovine serum, and with or without 4 mM folate³⁵ in an incubator with a humidified atmosphere (5% CO₂) at 37 $^{\circ}$ C. FA-PM or FI-PM was then added to the 6 well cell culture cluster dishes for 1 h at 37 $^{\circ}$ C. After incubation, the cells were washed with 0.01M (PBS) three times to remove unbound FA-PM or FI-PM and, the glass Bottom Cell Culture Dish cells were fixed in 4% formaldehyde and then stained with DAPI (1 μ g/ml), and the photoluminescence images of the cellular micelles were acquired by a laser scanning confocal microscope (LSCM, Leica TCS SP5, Germany). The 6 well cell culture cluster cell fluorescence intensity was analyzed by BD FACSVerser flow cytometry.

Data analysis

Statistical analysis was performed using Student's t-test for two groups by spss 11.0 software. All results were expressed as the mean \pm standard deviation (SD) unless otherwise noted.

Conclusions

The folate receptor expression in different phases of HeLa cells was investigated by flow cytometric and immunocytochemical methods in this study. Then, the effects of the cell cycle on the uptake of FI-PM and FA-PM by the HeLa cell line were studied by laser scanning confocal microscopy and flow cytometry. Based on the flow cytometric measurements for the G1, S and G2/M phase cell groups, we found that the cellular uptake of FI-PM in the G2/M phase was the highest, while the cellular uptake of FA-PM in the S phase was the highest. These results suggest that future studies on ligand mediated active targeting preparations should consider the cell cycle, especially when this system is used for cell cycle-specific drugs.

Acknowledgements

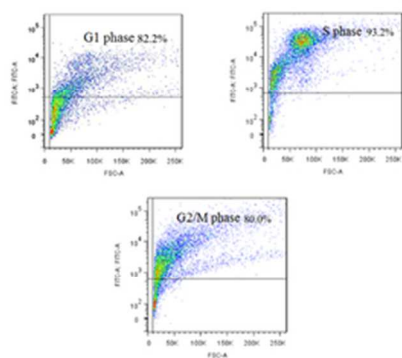
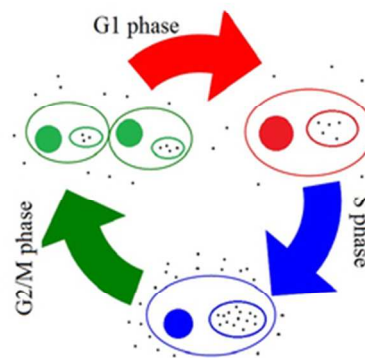
Financial support was received from the National Natural Science Foundation of China (81274100 and 81273469), Natural Science Foundation of Anhui Province of China (1408085QH189), Key Project for the Excellent Higher Education of Anhui Province of China (2013SQRL019ZD) and College Students Innovation and Entrepreneurship Science training plan (201410366040 and AH201410366119). Financial support was also provided by Young and middle-aged academic backbone from Anhui Medical University.

Notes and references

- 1 S. S. Suri, H. Fenniri and B. Singh, Nanotechnology-based drug delivery systems, *J. Occup. Med. Toxicol.*, 2007, **2**, 16.
- 2 E. Oh, J. B. Delehanty, K. E. Sapsford, K. Susumu, R. Goswami, J. B. Blanco-Canosa, P. E. Dawson, J. Graneek, M. Shoff, Q. Zhang, P. L. Goering, A. Huston and I. L. Medintz, Cellular Uptake and Fate of PEGylated Gold Nanoparticles Is Dependent on Both Cell-Penetration Peptides and Particle Size, *ACS. Nano.*, 2011, **5**(8): 6434-48.
- 3 X. Yi, X. Shi and H. Gao, Cellular uptake of elastic nanoparticles. *Phys. Rev. Lett.*, 2011, **107**(9): 098101.
- 4 E. Gravel, B. Thézé, I. Jacques, P. Anilkumar, K. Gombert, F. Ducongé and E. Doris, Cellular uptake and trafficking of polydiacetylene micelles. *Nanoscale*, 2013, **5**(5): 1955-60.
- 5 Z. Li, J. Hüve, C. Krampe, G. Luppi, M. Tsotsalas, J. Klingauf, L. De Cola and K. Riehemann, Internalization pathways of anisotropic disc-shaped zeolite L nanocrystals with different surface properties in HeLa cancer cells, *Small*, 2013, **9**(9-10): 1809-20.
- 6 J.A. Kim, A. Salvati, C. Åberg and K.A. Dawson, Suppression of nanoparticle cytotoxicity approaching in vivo serum concentrations: limitations of in vitro testing for nanosafety, *Nanoscale*, 2014, **6**(23): 14180-4.
- 7 D. Needham, H. P. Ting-Beall and R. Tran-Son-Tay, A Physical Characterization of GAP A3 Hybridoma Cells: Morphology, Geometry, and Mechanical Properties, *B. Biotechnol. Bioeng.*, 1991, **38**(8): 838-52.
- 8 M. P. Stewart, J. Helenius, Y. Toyoda, S. P. Ramanathan, D. J. Muller and A. A. Hyman, Hydrostatic pressure and the actomyosin cortex drive mitotic cell rounding, *Nature*, 2011, **469**(7329): 226-30.
- 9 M. A. Bach, D. E. Lewis, J. E. McClure, N. Parikh, H. M. Rosenblatt and W. T. Shearer, Monoclonal Anti-actin Antibody Recognizes a Surface Molecule on, Normal and Transformed Human B Lymphocytes: Expression, Varies with Phase of Cell Cycle, *Cell. Immunol.*, 1986, **98**(2): 364-74.
- 10 D. Needham, Possible Role of Cell Cycle-Dependent, Morphology, Geometry, and Mechanical, Properties in Tumor Cell Metastasis, *Cell Biophys.*, 1991, **18**(2): 99-121.
- 11 F. Bennett, A. Rawstron, M. Plummer, R. de Tute, P. Moreton, A. Jack and P. Hillmen, B-cell chronic lymphocytic leukaemia cells show specific changes in membrane protein expression during different stages of cell cycle, *Br. J. Haematol.*, 2007, **139**(4):600-4.
- 12 B. J. Keys, M. Hoyle and A. J. Millis, Cell cycle dependent expression of a glucose regulated cell surface glycoprotein, *In Vitro*, 1981, **17**(9): 769-76.
- 13 J. L. Urdiales, E. Becker, M. Andrieu, A. Thomas, J. Jullien, L. A. van Grunsven, S. Menut, G. I. Evan, D. Martín-Zanca and B. B. Rudkin, Cell Cycle Phase-Specific Surface Expression of Nerve Growth Factor Receptors TrkA and p75NTR, *J. Neurosci.*, 1998, **18**(17): 6767-75.
- 14 K. Takase, H. Okawa, K. Minato and J. Yata, Cell cycle-related expression of surface antigens on myelomonocytic leukemia cells, *Leuk. Res.*, 1988, **12**(7): 583-90.
- 15 D. Frey, V. Coelho, U. Petrausch, M. Schaefer, U. Keilholz, E. Thiel, and P. M. Deckert, Surface expression of gpA33 is dependent on culture density and cell-cycle phase and is regulated by intracellular traffic rather than gene transcription, *Cancer Biother. Radiopharm.*, 2008, **23**(1): 65-73.
- 16 J. L. Williams, J. W. Pickering and M. Wolcott, Selective cell surface expression of thymus leukemia antigen during S phase of the cell cycle, *J. Immunol.*, 1979, **122**(3): 1121-5.
- 17 M. O. Aksoy, Y. Yang, R. Ji, P. J. Reddy, S. Shahabuddin, J. Litvin, T. J. Rogers and S. G. Kelsen, CXCR3 surface expression in human airway epithelial cells: cell cycle dependence and effect on cell proliferation, *Am. J. Physiol. Lung Cell Mol. Physiol.*, 2006, **290**(5): L909-18.
- 18 C. R. Myers and M. L. Collins, Cell-cycle-specific fluctuation in cytoplasmic membrane composition in aerobically grown *Rhodospirillum rubrum*, *J. Bacteriol.*, 1987, **169**(12): 5445-51.
- 19 S. Zheng, J. Y. Chen, J. Y. Wang, L. W. Zhou and Q. Peng, Effects of cell cycle on the uptake of water soluble quantum dots by cells, *J. Appl. Phys.*, 2011, **110** (12):1-7.
- 20 J. A. Kim, C. Åberg, A. Salvati and K. A. Dawson, Role of cell cycle on the cellular uptake and dilution of nanoparticles in a cell population, *Nat. Nanotechnol.*, 2011, **7**(1): 62-8.
- 21 C. Åberg, J. A. Kim, A. Salvati and K. A. Dawson, Theoretical framework for nanoparticle uptake and accumulation kinetics in dividing cell populations, Theoretical framework for nanoparticle uptake and accumulation kinetics in dividing cell populations, *Europhys. Lett.*, 2013, **101**(3): 38007.
- 22 Y. Lu and P. S. Low, Folate-mediated delivery of macromolecular anticancer therapeutic agents, *Adv. Drug Deliv. Rev.*, 2002, **54**(5): 675-93.
- 23 B. L. Bohnsack and K. K. Hirschi, Nutrient regulation of cell cycle progression, *Annu Rev Nutr.*, 2004, **24**:433-53.
- 24 M. Srinivasarao, C. V. Galliford and P. S. Low Principles in the design of ligand-targeted cancer therapeutics and imaging agents, *Nat Rev Drug Discov.*, 2015, **14**(3):203-19.

Journal Name ARTICLE

- 25 Q. Tu, Y. Zhang, R. Liu, J. C. Wang, L. Li, N. Nie, A. Liu, L. Wang, W. Liu, L. Ren, X. Wang and J. Wang, Active drug targeting of disease by nanoparticles functionalized with ligand to folate receptor, *Curr. Med. Chem.*, 2012, **19**(19): 3152-62.
- 26 J. H. Tang, J. Yao, J. B. Shi, Q. P. Xiao, J. P. Zhou and F. H. Chen, Synthesis, characterization, drug-loading capacity and safety of novel pH-independent amphiphilic amino acid copolymer micelles, *Pharmazie*, 2012, **67**(9) : 756-764.
- 27 C. Wang, L. Qiao, Q. Zhang, H. Yan and K. Liu, Enhanced cell uptake of superparamagnetic iron oxide nanoparticles through direct chemisorption of FITC-Tat-PEG600-b-poly(glycerol monoacrylate), *Int. J. Pharm.*, 2012, **430**(1-2): 372-80.
- 28 D. Raucher and M. P. Sheetz, Membrane Expansion Increases Endocytosis Rate during Mitosis, *J. Cell Biol.*, 1999, **144**(3): 497-506.
- 29 M. Johansson and J. L. Persson, Cancer therapy: targeting cell cycle regulators, *Anticancer Agents Med. Chem.*, 2008, **8**(7): 723-31.
- 30 P. Zhang, Z. Zhang, Y. Yang and Y. Li, Folate-PEG modified poly(2-(2-aminoethoxy)ethoxy)phosphazene/DNA nanoparticles for gene delivery: Synthesis, preparation and in vitro transfection efficiency, *Int. J. Pharm.*, 2010, **392**(1-2) 241-8.
- 31 M. L. Whitfield, G. Sherlock, A. J. Saldanha, J. I. Murray, C. A. Ball, K. E. Alexander, J. C. Matese, C. M. Perou, M. M. Hurt, P. O. Brown and D. Botstein, Identification of genes periodically expressed in the human cell cycle and their expression in tumors, *Mol. Biol. Cell.*, 2002, **13**(6):1977-2000.
- 32 M. D. Forster, M. G. Ormerod, R. Agarwal, S. B. Kaye and A. L. Jackman, Flow Cytometric Method for Determining Folate Receptor Expression on Ovarian Carcinoma Cells, *Cytometry A.*, 2007, **71**(11): 945-50.
- 33 Y. Gao, M. Li, X. Zhang, T. Bai, G. Chi, J.Y. Liu and Y. Li, Isolation, culture and phenotypic characterization of human sweat gland epithelial cells, *Int. J. Mol. Med.*, 2014, **34**(4): 997-1003.
- 34 E. J. Go, E. J. Kim and W. Hur, In vitro cellular uptake of fibroin microspheres and its dependency on the cell cycle stage, *J. Microencapsul.*, 2013, **30**(2): 124-31.
- 35 H. Arima, A. Yoshimatsu, H. Ikeda, A. Ohyama, K. Motoyama, T. Higashi, A. Tsuchiya, T. Niidome, Y. Katayama, K. Hattori and T. Takeuchi, Folate-PEG-appended dendrimer conjugate with α -cyclodextrin as a novel cancer cell-selective siRNA delivery carrier, *Mol. Pharm.*, 2012, **9**(9): 2591-604.

Expression of FR- α in different cell cycle**Uptake folate modified poly(L-amino acids) micelles**

55x25mm (300 x 300 DPI)